Defining a tandem repeat catalog and variation clusters for genome-wide analyses

Ben Weisburd,*[,#1,2] Egor Dolzhenko,*[,#3] Mark F. Bennett,[4,5,6] Matt C. Danzi,[7] Isaac R. L. Xu,[7] Hope Tanudisastro,[8-11] Adam English,[12] Laurel Hiatt,[13] Tom Mokveld,[3] Guilherme De Sena Brandine,[3] Nehir Edibe Kurtas,[2,1] Helyaneh Ziaei Jam,[14] Harrison Brand,[2,1] Stephan Züchner,[7] Melissa Gymrek,[14] Harriet Dashnow,[15] Michael A. Eberle,*[3] Heidi L. Rehm*[1,2]

* equal contribution, [#] corresponding authors

1. Program in Medical and Population Genetics, Broad Center for Mendelian Genomics, Broad Institute of MIT and Harvard, Cambridge, MA, USA
2. Center for Genomic Medicine, Massachusetts General Hospital, Harvard Medical School, Boston, MA, USA
3. Pacific Biosciences, 1305 O'Brien Drive, Menlo Park, CA, USA
4. Population Health and Immunity Division, Walter and Eliza Hall Institute of Medical Research, Parkville, Victoria, Australia
5. Department of Medical Biology, University of Melbourne, Parkville, Victoria, Australia
6. Epilepsy Research Centre, Department of Medicine, University of Melbourne, Austin Health, Heidelberg, Victoria, Australia
7. Dr. John T. Macdonald Foundation Department of Human Genetics and John P. Hussman Institute for Human Genomics, University of Miami Miller School of Medicine, Miami, FL, USA
8. Centre for Population Genomics, Garvan Institute of Medical Research, Sydney, NSW, Australia
9. Centre for Population Genomics, Murdoch Children's Research Institute, Melbourne, VIC, Australia
10. Faculty of Medicine and Health, University of New South Wales, Sydney, NSW, Australia
11. Faculty of Medicine and Health, University of Sydney, Sydney, NSW, Australia
12. Human Genome Sequencing Center, Baylor College of Medicine, Houston, TX, USA
13. University of Utah, Department of Human Genetics, Salt Lake City, UT
14. Department of Computer Science and Engineering, University of California San Diego, La Jolla, CA
15. Department of Biomedical Informatics, University of Colorado Anschutz Medical Campus, Aurora, CO

Abstract

Tandem repeat (TR) catalogs are important components of repeat genotyping studies as they define the genomic coordinates and expected motifs of all TR loci being analyzed. In recent years, genome-wide studies have used catalogs ranging in size from fewer than 200,000 to over 7 million loci. Where these catalogs overlapped, they often disagreed on locus boundaries, hindering the comparison and reuse of results across studies. Now, with multiple groups developing public databases of TR variation in large population cohorts, there is a risk that, without sufficient consensus in the choice of locus definitions, the use of divergent repeat catalogs will lead to confusion, fragmentation, and incompatibility across future resources.

In this paper, we compare existing TR catalogs and discuss desirable features of a comprehensive genome-wide catalog. We then present a new, richly annotated catalog designed for large-scale analyses and population databases. Our catalog stratifies TRs into two groups: 1) isolated TRs suitable for repeat copy number analysis using short-read or long-read data and 2) so-called variation clusters that contain TRs within wider polymorphic regions that are best studied through sequence-level analysis. To define variation clusters, we present a novel algorithm that leverages long-read HiFi sequencing data to group repeats with surrounding polymorphisms. We show that the human genome contains at least 25,000 complex variation clusters, most of which span over 120 bp and contain five or more TRs. Resolving the sequence of entire variation clusters instead of individually genotyping constituent TRs leads to a more accurate analysis of these regions and enables us to profile variation that would have been missed otherwise.

Introduction

Tandem repeats (TRs) are nucleotide sequences composed of consecutive repetitions of a shorter motif (also called a repeat unit). TRs with motif size of 6 bp or less are called short tandem repeats (STRs) while those with longer motifs are called variable number tandem repeats (VNTRs). These sequences can be perfect repeats of a single motif - for example CAG CAG CAG CAG, or they can contain interruptions - as in CAG CAG CAA CAG. Over the past fifteen years, wide-ranging biological studies have used sequencing data to investigate many aspects of TRs including mutation rates,[1–4] effects on gene expression,[5] splicing,[6] and disease risk.[7,8] With the exception of several specialized methods for identifying *de novo* variation,[9–11] most TR genotyping tools[12–21] involved in these studies require the user to provide a TR catalog which specifies the reference coordinates and motifs of each TR locus to genotype - making the choice of catalog a key factor in the overall sensitivity of a study.[22–24]

Researchers have typically generated TR catalogs using tools like Tandem Repeats Finder (TRF)[25] that detect repetitive sequences by scanning the reference genome. Although a reference-based approach is able to identify a wide range of TR loci, it can miss polymorphic repeats that are too short or absent from the reference genome. Furthermore, methods like TRF are highly sensitive to input parameters, with some commonly-used settings yielding fewer than 1 million mostly perfect TRs, while other settings produce over 10 million TRs that contain many sequence interruptions. An alternative approach, which we call the cohort-driven strategy, detects TR variation directly from the sequencing data[9,10,26] or haplotype-resolved assemblies.[27,28] The cohort-driven strategy not only prioritizes polymorphic loci, but can also capture TRs that are not well represented in the reference genome and hence missed by the reference-based approach.

In addition to the different strategies for identifying TR loci, another important aspect of catalog design is the definition of locus boundaries. Since naturally occurring repeat sequences can contain interruptions or consist of multiple arrays of highly similar motifs, defining the starts and ends of TR loci in the reference genome is often subject to ambiguity. Yet, even small, seemingly inconsequential differences in how locus boundaries are specified within different catalogs, resources, or reference materials can lead to real issues with interpretation of TR genotypes. For example, the *PABPN1* locus has two commonly used definitions. With narrower locus boundaries, the pathogenic threshold is 8 GCGs, while with wider boundaries, it becomes 12 GCGs, creating the potential for inadvertent errors in the diagnosis of autosomal dominant oculopharyngeal muscular dystrophy (OPMD) if the genotype (number of repeats) is interpreted without awareness of which locus definition was used when running the genotyping tool (**Supplementary Information**).

The selection of TR loci and the specification of their boundaries can influence the suitability of a catalog for two different kinds of downstream analysis approaches. The first approach focuses primarily on the quantification of repeat copy numbers and using them to detect outlier expansions or perform association tests with other variables like gene expression. The second approach involves sequence-level analysis of TR regions in order to characterize motif composition, interruption patterns, and properties of flanking sequences. Most existing TR genotyping tools, especially those designed for short-read data, only report repeat copy numbers and not allele sequences.[12,13] They are unable to resolve the full sequence-level variations of complex regions such as nested repeats and repeats surrounded by other repeats or structural variants.[29] Additionally, these tools work best with narrow locus definitions that contain only perfect or nearly-perfect repeat sequences.[28] Therefore, catalogs designed for repeat copy number analysis benefit from setting narrow locus boundaries, and flagging or excluding

TRs within complex regions. On the other hand, the latest generation of tools[14,15,21] can report allele sequences in addition to repeat copy numbers, and so enables sequence-level analysis both for isolated TRs as well as more complex repeat regions.[30,31] Examples of TR variation that especially benefit from sequence-level analysis include the recently identified polymorphic region associated with the stability of the FGF14 repeat,[32] a single base pair insertion in a homopolymer located within a *MUC1* VNTR that causes autosomal dominant tubulointerstitial kidney disease (ADTKD), and TRs like the *RFC1* locus whose pathogenicity is affected by sequence composition changes.[33,34] Such loci frequently correspond to fragments of perfect tandem repeats punctuated by insertions, deletions, and substitutions in and around the repeat sequence.

Taken together, these observations highlight the challenges of creating genome-wide TR catalogs suitable for population studies, especially multi-center studies employing different computational tools and sequencing technologies. To help address these challenges, we introduce a new genome-wide repeat catalog. We employ both cohort-based and reference-based TR identification approaches to capture a comprehensive set of loci, including those that harbor common or rare variation. To simplify adoption, we share the catalog in the different formats used by popular TR analysis tools for short- and long-read data. Our catalog also stratifies TRs into two groups: isolated TRs suitable for repeat copy number analysis and variation clusters that contain TRs surrounded by polymorphic sequence. Due to their complexity, variation clusters are best studied through sequence level analysis, particularly using long-read data. To perform this stratification we introduce a new method for profiling population-scale variation around TRs and other regions of the genome. Lastly, we share the trexplorer.broadinstitute.org web portal to enable interactive online exploration of the loci and variation clusters in our catalog. Users can view TR population allele frequency distributions, visualize locus boundaries, and filter TRs by various criteria such as genomic interval, gene name, repeat motif, and/or polymorphism rate. Among other things, the filtering functionality allows users to define a smaller subset of the catalog that is most relevant to their particular study objectives, and then export it in the file format required as input to their preferred TR genotyping tool.

Results

Existing tandem repeat catalogs

Widely-used TR catalogs differ substantially in their core attributes such as their total number of loci, range of included motif sizes, and repeat purity (**Table 1**, **Figure 1**, **Figures S1, S2, Methods**). Strikingly, pairwise comparison of eleven TR catalogs

showed that every pair differed in over half of their TR definitions (**Figure S1**). Many of these catalogs were aimed at different study objectives, tools and sequencing technologies, and so used different minimum repeat length and purity thresholds when selecting TR loci for inclusion. Also, they employed distinct approaches to define locus boundaries. For example, the recently-released Adotto v1.2, Platinum TRs v1.0, and the Chiu et al. 2024 catalogs contain many long imperfect repeats and include non-repetitive flanking sequences. Such locus definitions are compatible with existing tools for genotyping TRs in long reads, but cannot be accurately genotyped with existing tools for short-read sequencing data. On the other hand, older catalogs like GangSTR v17 and Illumina 174k define narrow locus boundaries around mostly perfect TR sequences and so are suitable for both short-read and long-read analyses. However, for technical or historical reasons, these catalogs have relatively low sensitivity as measured by their degree of overlap with our test set of true positive polymorphic STR loci with 3-6 bp motifs (**Methods**).

row	catalog	total loci	genome coverage	motif sizes	locus sizes in reference	pure repeat fraction in reference	includes chrX	includes chrY	polymorphic STRs missed
1	Known disease-associated TRs + adjacent repeats & historical candidate loci	83	<0.01%	1 - 27 bp	6 - 150 bp	94%	✓	x	N/A
2	Illumina 174k polymorphic loci	174,286	0.15%	1 - 24 bp	4 - 532 bp	100%	✓	x	71%
3	UCSC Simple Repeat Track	965,511	9.9%	1 - 1,991 bp	13 - 499,998 bp	83%	✓	✓	38%
4	Vamos v2.1	1,243,954	2.9%	1 - 667 bp	1 - 9,975 bp	64%	✓	✓	27%
5	GangSTR v17	1,340,266	0.74%	1 - 20 bp	10 - 612 bp	100%	✓	✓	53%
6	HipSTR	1,638,945	1.4%	1 - 6 bp	9 - 132,210 bp	77%	✓	✓	30%
7	Adotto v1.2 *	2,934,805	3.9%	1 - 495 bp	4 - 49,802 bp	85%	✓	✓	13%
8	popSTR	5,401,401	2.7%	1 - 6 bp	8 - 136 bp	96%	x	x	26%
9	Platinum TRs v1.0 **	† 7,524,815	5.1%	1 - 822 bp	4 - 9,504 bp	90%	✓	✓	45%
10	Chiu et al. 2024	18,759,399	10.7%	2 - 100 bp	2 - 185,860 bp	70%	✓	x	4%

Table 1: Properties of commonly-used TR catalogs, including the total size, total span, and motif size ranges. The “Polymorphic STRs missed” column is based on lack of overlap with a test set of 250,262 polymorphic STRs with 3-6 bp motifs identified in 78 diverse haplotype-resolved assemblies. Overlap was defined leniently as having any TR definition that overlapped the test set STR by 1 bp or more, regardless of motif.

* For the Adotto v1.2 catalog, each of the original 1,784,804 entries was split into its constituent TRs, before calculating statistics
** The PlatinumTR v1.0 catalog was converted from TRGT catalog format, splitting any compound locus definitions into their constituent TRs (**Methods**). † 296,782 loci (3.8%) were excluded because their reference sequences contained interruptions that prevented us from unambiguously splitting the region into its constituent repeats.

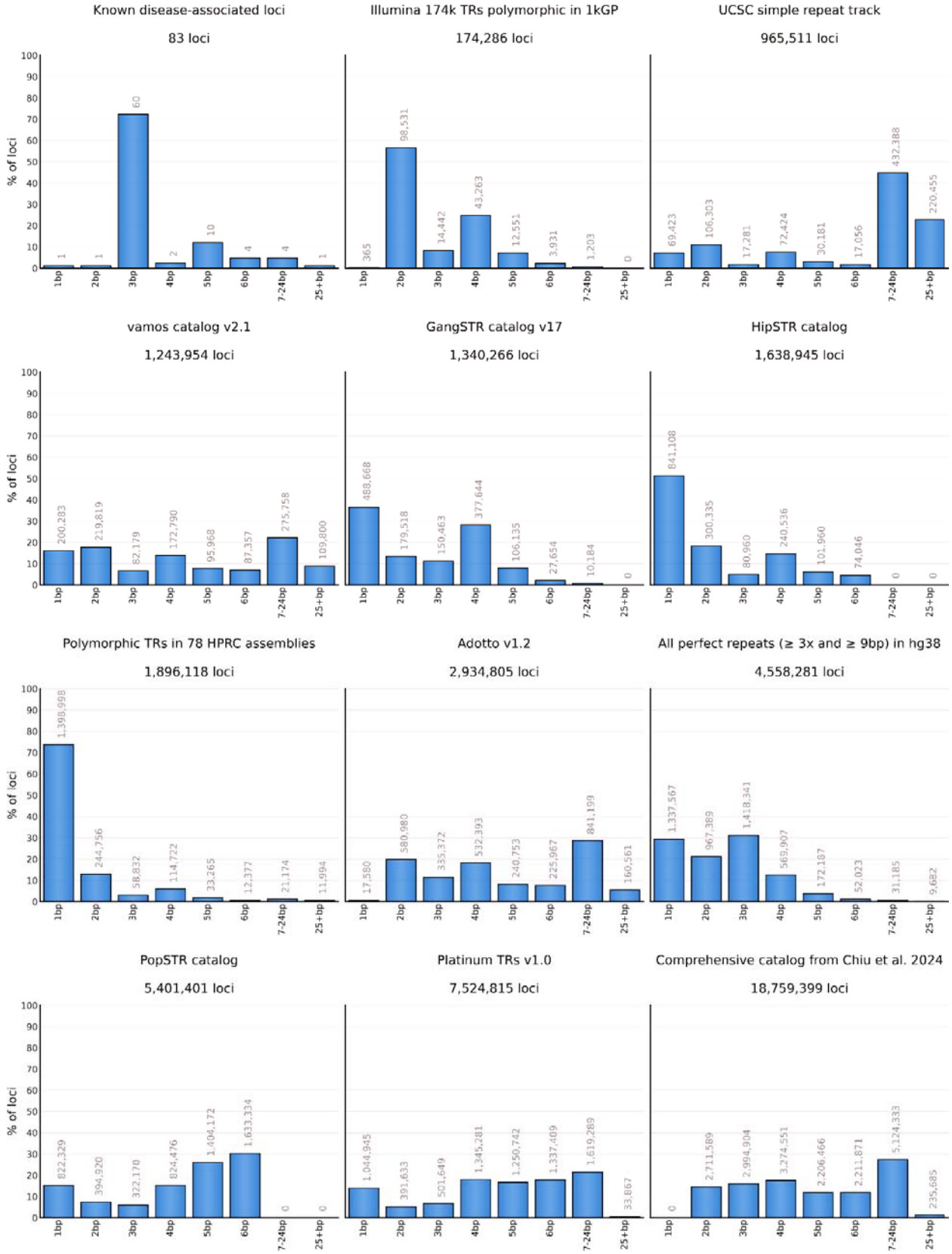
Known disease-associated loci
83 loci
Illumina 174k TRs polymorphic in 1kGP
174,286 loci
UCSC simple repeat track
965,511 loci
vamos catalog v2.1
1,243,954 loci
GangSTR catalog v17
1,340,266 loci
HipSTR catalog
1,638,945 loci
Polymorphic TRs in 78 HPRC assemblies
1,896,118 loci
Adotto v1.2
2,934,805 loci
All perfect repeats (≥ 3x and ≥ 9bp) in hg38
4,558,281 loci
PopSTR catalog
5,401,401 loci
Platinum TRs v1.0
7,524,815 loci
Comprehensive catalog from Chiu et al. 2024
18,759,399 loci
% of loci
1bp
2bp
3bp
4bp
5bp
6bp
7-24bp
25+bp
1 1 60 2 10 4 4 1
365 58,531 14,442 43,263 12,551 3,931 1,203 0
69,423 106,303 17,281 72,424 30,181 17,056 432,388 220,455
200,283 219,819 82,179 172,790 95,968 87,357 275,758 109,800
488,668 179,518 150,463 377,644 106,135 27,654 10,184 0
841,108 300,335 80,960 240,536 101,960 74,046 0 0
1,398,998 244,756 58,832 114,722 33,265 12,377 21,174 11,994
17,580 580,980 335,372 532,393 240,753 225,967 841,199 160,561
1,337,567 967,389 1,418,341 569,907 172,187 52,023 31,185 9,682
622,329 394,920 322,170 624,476 1,404,172 1,633,334 0 0
1,044,945 391,633 501,649 1,345,281 1,250,742 1,337,409 1,619,289 33,867
0 2,711,589 2,994,904 3,274,551 2,206,466 2,211,871 5,124,333 235,685

Figure 1. Comparison of motif size distributions across TR catalogs. The x-axis represents motif sizes. Each bar is labeled with the number of loci it contains.

Defining a genome-wide catalog

To incorporate the advantages of both reference-based and cohort-driven approaches, we collected loci from three cohort-driven catalogs and one reference-based catalog (**Table 2**). Where multiple source catalogs contained different definitions of the same TR locus (**Methods**), the higher prioritized definition - as described in Table 2 - was incorporated. To preserve compatibility of our locus definitions with those of existing resources, we prioritized widely-used catalogs above those from the new TR sources introduced in this paper. First, we included 63 disease-associated loci, 10 of their adjacent repeats, as well as 10 candidate TR loci that have been historically included in rare disease analyses. These loci have been the focus of extensive research,[35,36] and many have well established, widely-used locus definitions which we incorporated here. Next, we added 174,244 loci from the Illumina catalog of polymorphic TRs which was created in 2021 by analyzing signals of TR variation within short-read sequencing data from 2,504 individuals in the 1000 Genomes Project.[26] Prioritizing this catalog above catalogs 3 and 4 (**Table 2**) ensured compatibility with the locus boundary definitions used in prior studies and resources.[37]

To ensure comprehensive inclusion of perfect repeat sequences, we identified all TRs in hg38 that spanned at least 3 copies of a 3-1000 bp motif, at least 5 copies of a dinucleotide motif, or at least 9 copies of a homopolymer motif (**Methods**). This contributed another 4,391,197 loci to our catalog. Our focus on perfect repeats was motivated by their higher mutation rates compared to interrupted repeats, their importance to TR-associated disease mechanisms,[38] as well as their higher overall genotyping accuracy in short-read analyses.[13] We chose a ≥ 3x threshold to match several known disease-associated loci such as *C9orf72* that span only three repeats in the hg38 reference. Additionally, this threshold represented a favorable trade-off between sensitivity and specificity in terms of capturing as many polymorphic TR loci as possible while not including too many loci overall (Fig. S2 in Weisburd et al. 2023).[28]

Finally, we incorporated polymorphic TRs detected using 78 haplotype-resolved T2T assemblies from the Human Pangenome Reference Consortium (HPRC) and Human Genome Structural Variation Consortium (HGSVC). The specialized method we

employed for this (**Methods**) allowed us to complement the previous three catalogs by capturing polymorphic loci that had fewer than three repeats in the reference, or that contained single base interruptions like those observed at known disease-associated loci such as *ZIC3*, *ATXN1, and FXN*. This approach contributed a further 297,519 TRs to the final catalog.

priority	catalog	total loci	genome coverage	motif sizes	locus sizes in reference	pure repeat fraction in reference	includes chrX	includes chrY	loci contributed to final catalog
1	Known disease-associated TRs + adjacent repeats & historical candidate loci	83	<0.01%	1 - 27 bp	6 - 150 bp	94%	✓	x	83
2	Illumina 174k polymorphic TRs in 1kGP	174,286	0.15%	1 - 24 bp	4 - 532 bp	100%	✓	x	174,244
3	Perfect repeats that span ≥ 9 bp and ≥ 3 repeats in hg38	4,558,281	2.0%	1 - 833 bp	9 - 2,523 bp	100%	✓	✓	4,391,197
4	Polymorphic TRs in 78 T2T assemblies	1,937,805	1.0%	1 - 833 bp	1 - 2,499 bp	100%	✓	✓	297,517
	Tandem Repeat Catalog	4,863,041	2.1%	1 - 833 bp	1 - 2,523 bp	100%	✓	✓	

Table 2: Four source catalogs that were incorporated into our tandem repeat catalog.

The resulting catalog contained 4,863,041 TRs that collectively spanned 2.1% of the hg38 reference. 4,803,366 of these (98.8%) were STRs, including 1,567,337 homopolymers (32.2%), 978,972 dinucleotide repeats (20.1%), 1,432,117 trinucleotide loci (29.4%), 590,787 loci with 4bp motifs (12.1%), 177,422 loci with 5bp motifs (3.6%), and 56,731 loci with 6bp motifs (1.2%). 59,675 were VNTRs (1.2%): 43,996 (0.9%) had 7 to 24 bp motif sizes and 15,679 (0.3%) had 25bp to 833bp motifs. Intersecting the catalog with Gencode v46 gene annotations and taking the most significant gene region based on the following priority: coding region (CDS), 5' untranslated region (UTR), 3' UTR, exon, intron, promoter, showed that 2,687,339 (55.3%) TRs in the catalog were intronic, 1,950,456 (40.1%) were intergenic, 56,725 (1.2%) overlapped promoters, 57,198 overlapped 3’ UTRs (1.2%), 54,883 (1.1%) overlapped exons of non-coding genes, 39,872 (0.8%) overlapped coding regions, and 16,568 (0.3%) overlapped 5’ UTRs.

Analysis of variation clusters

Some tandem repeats (TRs) are located within regions that have high rates of polymorphism and hence often differ significantly from the reference genome (**Figure 2 A-C**). We refer to such regions as variation clusters (VCs). Because most methods for TR analysis assume that the regions surrounding the TR closely resemble the reference genome, TRs located within variation clusters may be prone to analysis errors. For example, consider (AT)n repeats located in a variation cluster in the *KCNMB2* gene (**Figure 2D**). In the individual shown, the flanks of these TRs significantly differ from the reference genome, making it difficult to locate the exact boundaries or separate one repeat from the other repeats located within this region. This issue can be avoided if we locate the boundaries of the entire VC and then determine its full-length allele

sequences in each sample with tools like TRGT[15] or LongTR.[14] Then the resulting sequences can be either analyzed directly or their repeat content can be characterized with existing methods,[15] making it possible to analyze VCs together with isolated TRs.

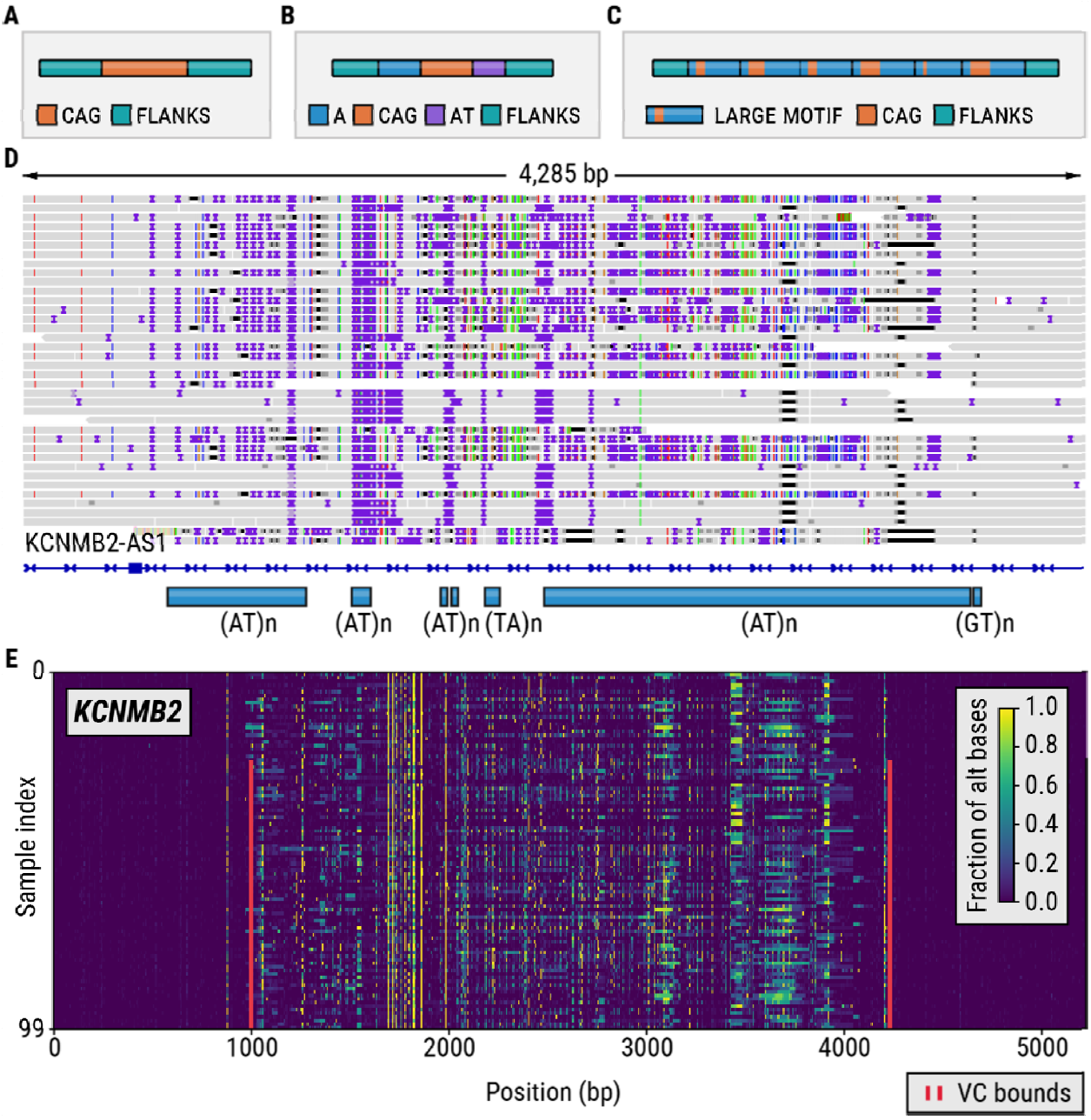

Figure 2: (A) A TR surrounded by non-repetitive flanks. (B) A TR with a CAG motif surrounded by an A homopolymer and AT dinucleotide repeat. (C) Nested TRs. (D) HiFi reads originating from the HG002 sample spanning a variation cluster located in an intron of the *KCNMB2* gene. (E) A variation plot depicting the *KCNMB2* locus in 100 long-read HiFi samples.

We developed a method, vclust, that when given a set of TR regions and aligned sequencing data from multiple samples can identify the bounds of variation clusters around each TR (**Methods**). We first used vclust to characterize variation across 63 loci containing known disease-associated TRs in 100 HiFi WGS HPRC samples. Our method identified variation clusters around eight of these TRs located in the *ATXN8OS*, *FGF14*, *NOP56*, *CNBP*, *HTT*, *BEAN1*, *LRP12*, and *EIF4A3* genes. Variation around most of these TRs has already been identified: the *ATXN8OS*, *NOP56*, *CNBP*, and *HTT* TRs contain adjacent repeats that contribute to variation in their flanks. A common insertion flanking the *FGF14* TR was recently found to have a stabilizing effect on this repeat.[32] As anticipated, the vclust analysis incorporated the site of this insertion into the *FGF14* variation cluster (**Figure 3A**). The *CNBP* and *NOP56* repeats were the only two known pathogenic TRs whose variation clusters extended the original TR region by more than 40 bp. The *CNBP* VC (**Figure 3B**) includes two polymorphic repeats with CAGA and CA motifs while the *NOP56* VC (**Figure 3C**) contains a common deletion located less than 50 bp away from the repeat boundary. *BEAN1*, *LRP12*, and *EIF4A3* VCs were caused by the presence of small indels adjacent to these repeats.

Next, we applied the variation cluster analysis to our catalog of 4,863,043 TRs. This analysis yielded 273,112 VCs that cumulatively overlapped 744,458 TRs, with 66% of VCs overlapping two or more TRs. About 18% of VCs (N=50,557) spanned over 120 bp in the reference (**Figure 4A**), a length at which exact genotyping with short-read data (30x 150bp WGS) becomes difficult. To demonstrate the benefits of genotyping complete variation clusters instead of constituent TRs, we compared the accuracy of allele sequences derived by genotyping entire VCs to the accuracy of alleles derived by genotyping the individual TRs in a long-read HiFi sequencing dataset from the HG002 sample. We defined accuracy as base-level concordance with a highly accurate assembly of the same genome [39,40] (**Methods**). The allele concordance rate increased from 79.43% for TRs (87.30% accepting off-by-one errors as concordant calls) to 90.58% (95.98%) for the corresponding VCs. The concordance rate was 96.21% (98.50%) for isolated TRs, demonstrating that individual TRs within VCs were a major source of genotyping errors. To further investigate VCs that contain multiple repeat tracts, we identified 24,867 VCs each containing five or more constituent TRs. We refer to these variation clusters as complex VCs. Complex VCs cumulatively contain 254,879 TRs, their median length is 208 bp and 86% exceed 120 bp (**Figure 4B**). For example, a VC in the *KCNMB2* gene (**Figure 2E**) spans over 3 Kbp in the reference genome and contains 135 TRs, including 116 TRs with either AT motifs.

We investigated the distribution of features that differed between isolated TRs compared to those within VCs or complex VCs (**Figure 5**). The majority of TRs with 1-9

bp repeat motifs are isolated TRs (88%), with this trend being most pronounced for homopolymer and trinucleotide TRs (93% and 94%, respectively). In contrast, only 34% of TRs with motifs 10 bp or larger are isolated TRs, while nearly half (46%) are located within complex VCs (**Figure 5A**). We also observed a higher proportion of isolated TRs in coding or untranslated regions (94%) relative to intronic, promoter, or intergenic regions (88%). Conversely, a higher percentage of TRs in intronic, promoter, or intergenic regions lie within complex VCs (5%) compared to those in coding or untranslated regions (1%) (**Figure 5B**). Finally, we found that TRs within VCs tend to have lower mappability while TRs with high mappability are nearly all isolated TRs (**Figure 5C**).

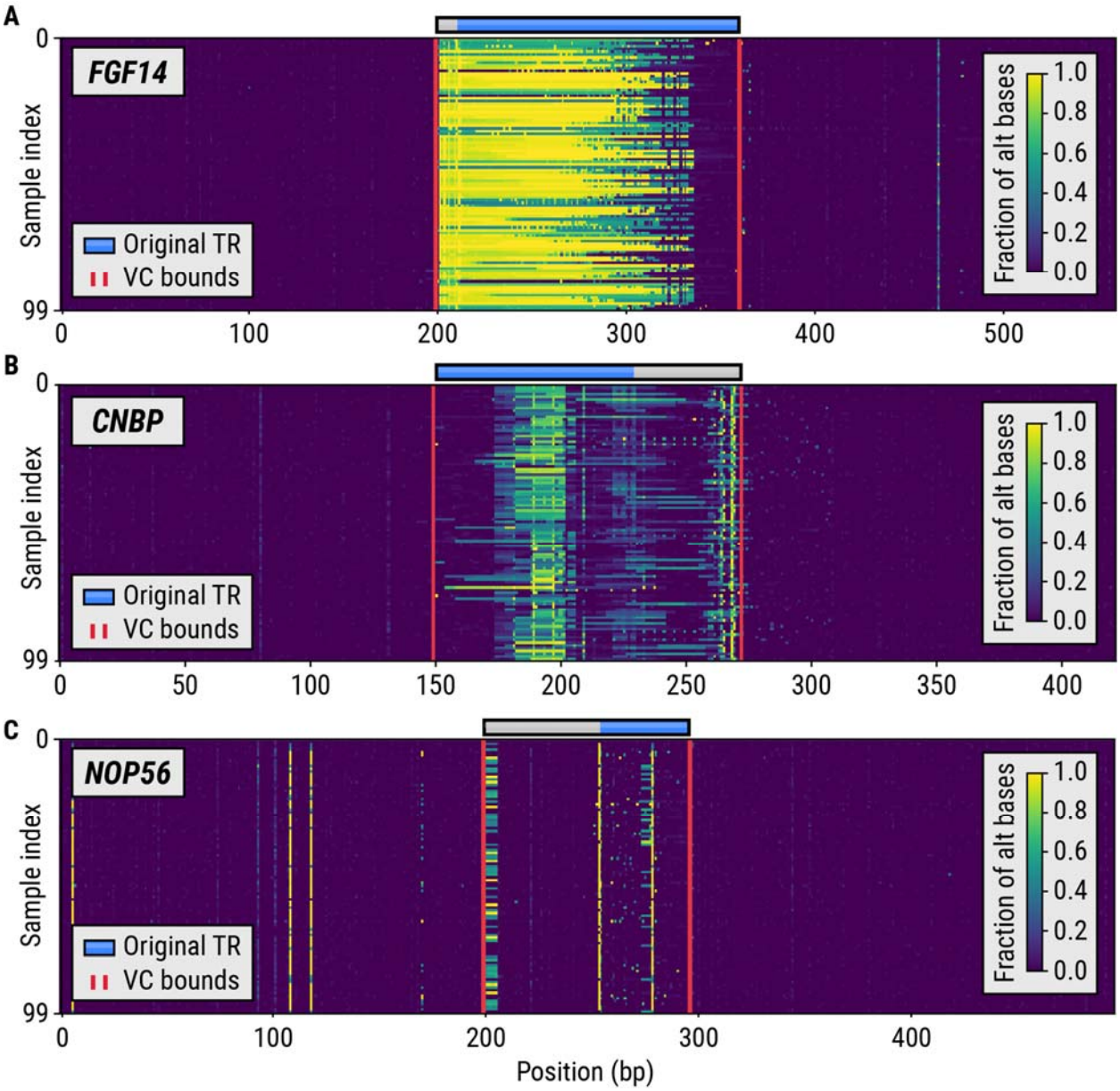

Figure 3. Variation plots showing the genetic variation in 100 HiFi HPRC samples

around known pathogenic repeats in the (A) *FGF14*, (B) *CNBP*, and (C) *NOP56* genes. The blue bars denote the boundaries of the original repeat region while the gray bars depict the extension of the repeat region to a full-length variation cluster.

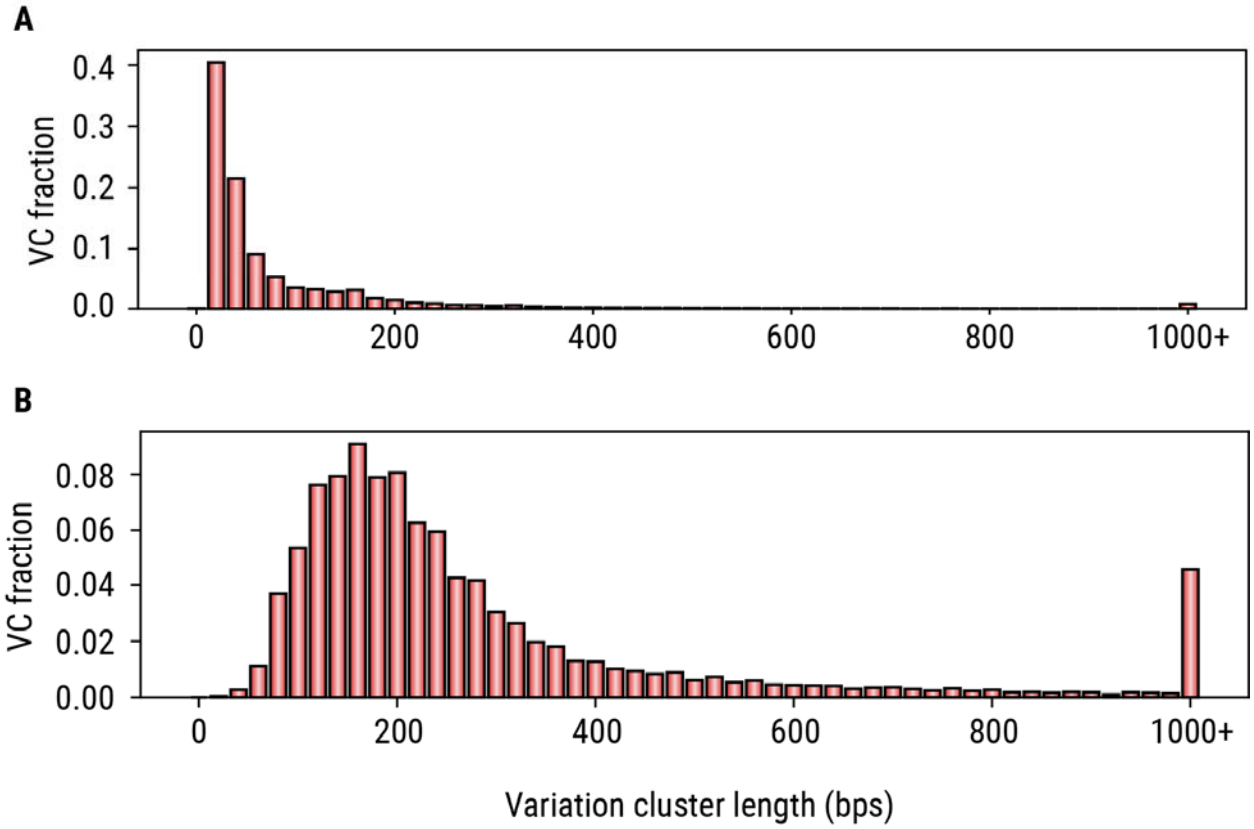

Figure 4. Size distributions of variation clusters. (A) Distribution of the differences between variation cluster length and the length of the original TR region that seeded it. (B) Distribution of lengths of complex variation clusters in the reference genome.

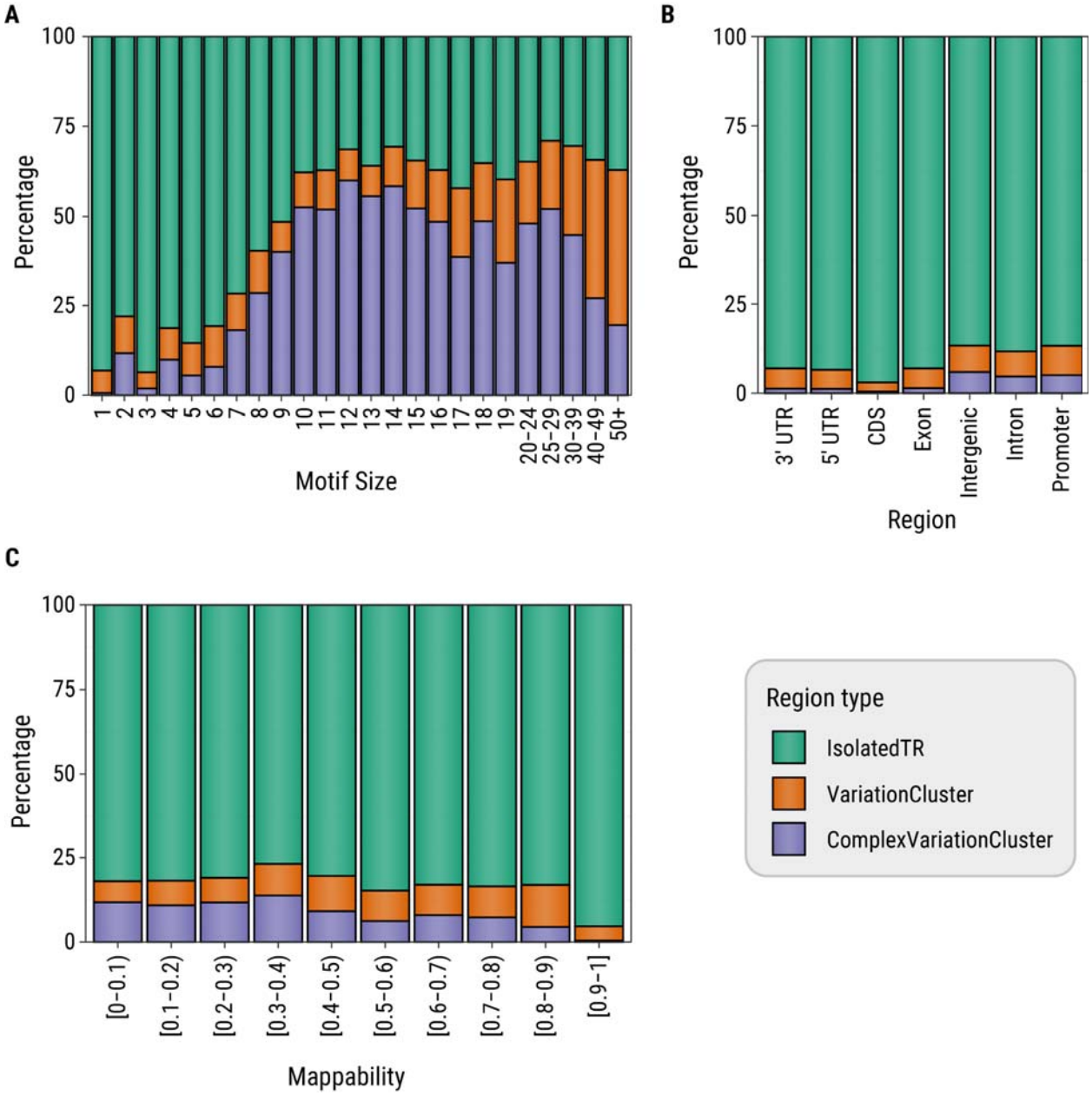

Figure 5. Percentage of tandem repeat (TR) loci in each variation cluster (VC) status group as a function of (A) motif size (in bp), (B) Gencode genomic region, and (C) mappability of tandem repeat locus and flanks. Isolated TRs are TRs that do not lie within a VC, complex VCs are VCs that contain five or more TRs.

Catalog Annotations and Utilities

To simplify the analysis of TRs in our catalog, we annotated them with several different categories of information, including their relationship to variation clusters, their gene

regions based on Gencode[41], Refseq[42] and MANE[43], the mappability of the TR loci and their flanking regions, and population allele frequencies derived from 78 haplotype-resolved assemblies from the HGDP and HGVSC consortia. Mappability for each TR was computed by taking the per-base scores from the 36-mer mappability track in the UCSC browser[44] and averaging them across the repeat locus and 150bp flanks. The UCSC 36-mer mappability score for a given genomic position represents the fraction of 36bp k-mers overlapping that position that are uniquely mappable in the genome. Although 36bp is much smaller than the typical short read length, we chose this k-mer size because it provides a more sensitive estimate of mappability than larger k-mer sizes and is particularly relevant to the mappability of spanning and flanking reads that include only a small amount of flanking sequence, and that short read genotyping tools rely on to estimate repeat allele sizes. These annotations are currently available in JSON format for all loci in the catalog (**Table S1**). As an illustration of their utility, we used these annotations to summarize the basic properties of known disease-associated loci (**Table S2**) and to reproduce Figure 2 in Danzi et al. 2025[45] which shows that many known disease-associated loci have some of the highest polymorphism rates among TR loci genome-wide (**Figure S4**).

Additionally, we share the *str-analysis* library of scripts and utilities for performing common operations on the catalog, such as filtering based on the above annotations, combining it with other TR catalogs, and computing various statistics (**Code Availability**).

Discussion

Advances in sequencing technologies and genotyping tools may soon make TR analysis a standard part of rare and common disease discovery pipelines alongside SNVs, indels and SVs. We expect that this will involve a transition from the current variety of highly custom, specialized approaches to a small number of well-established methods and repeat catalogs. The lack of consensus around TR catalog design in particular may become increasingly problematic as population databases and other large-scale surveys of TR variation are made available. Our study is therefore an effort to build consensus by bringing issues and trade-offs involved in TR catalog design to the foreground.

While existing genome-wide TR catalogs have enabled a range of important discoveries, they are still primarily designed for specific tools and sequencing technologies that make them suboptimal choices for population resources of TR variation. Although newer catalogs[2,27,46] cover a large fraction of repeats in the human genome, they use permissive locus definitions that include significant amounts of non-

repetitive sequence. Such catalogs cannot be easily applied to studies based on short-read data which will remain important due to the wide-spread adoption and larger sample sizes of these datasets. Many older catalogs developed for short-read tools do support repeat copy number analyses in both short-read and long-read data. However, these catalogs remain incomplete, missing a substantial fraction (30% or more) of the polymorphic STR loci in our test sets.

We therefore developed a catalog that incorporates TRs identified in the reference genome as well as polymorphic TRs detected through cohort-based analyses, ensuring comprehensive representation of a wider range of TR loci that are amenable to both short-read and long-read analysis. To simplify adoption, we provide the catalog in the different formats expected by short-read and long-read tools. Additionally, we annotate the TR loci with their gene regions, population allele frequencies from 78 T2T assemblies, and other properties. Our catalog stratifies TRs into two groups: isolated TRs and variation clusters. This second group is derived using a novel tool that extends the boundaries of TRs located within broader regions of variation. This is similar to how HipSTR and LongTR dynamically extend the repeat boundaries when variation is detected close to the original repeat region. While the HipSTR/LongTR approach improves genotyping accuracy, it can lead to discordant repeat definitions when these tools are applied to different sample batches because the boundaries are adjusted at genotyping time. In contrast, defining variation cluster boundaries apriori with our new tool vclust facilitates comparisons across studies/batches in downstream analyses.

We hope that the TR catalog and the computational tools introduced in this paper will serve as a starting point for a dynamic community resource that will address the needs of most research groups involved in profiling variation in TR regions. The adoption of a shared catalog across TR studies and population databases will help avoid future challenges in the reuse and interpretation of TR analysis results, including population allele frequencies and pathogenic thresholds.

Going forward, we will extend the catalog by adding TR loci not captured by our current approach. This includes a broader set of polymorphic VNTRs and interrupted repeats. For each locus, our catalog currently specifies only the TR motifs present in the reference genome, it will be important to supplement our TR definitions with motif sets observed in other genomes.[19,47] Future work will characterize the accuracy of TR genotypes across loci, tools, and sequencing technologies to identify loci that can be accurately genotyped using short-read tools as well as those loci that can only be resolved using long reads. The catalog would also benefit from annotations related to methylation states, interruption patterns, somatic mosaicism, and most importantly, population allele frequencies derived from larger sample sizes.

Methods

Catalog comparison

All catalog comparison steps were implemented in the tandem-repeat-catalogs GitHub repo compare_catalogs.py script. Prior to comparison, any compound locus definitions were split into their constituent TR loci, each of which had a single chromosome, start (0-based), end, and motif. For example, the compound definition of the *HTT* locus described by the expression (CAG)*CAACAG(CCG)* would be split into two separate definitions with the motifs CAG and CCG. For the Vamos v1.2 catalog, the first motif was selected from each motif set. The PlatinumTRs v1.0 TRGT catalog contained compound locus definitions that typically spanned multiple adjacent TRs without specifying the boundaries between them. To use the same approach for all catalogs, we attempted to split these compound definitions into their constituent TRs by locating stretches of perfect repeats of each specified motif within the reference sequence, as implemented in the str-analysis repo convert_trgt_catalog_to_expansion_hunter_catalog.py script. For 296,782 out of 7,722,729 locus definitions (3.8%), the exact boundaries of constituent TRs couldn't be resolved in this way due to interruptions in the reference sequence, so we excluded them from comparisons and statistics.

In Table 1, comparison of each catalog with the test set of polymorphic STRs was performed by converting the catalogs to BED format, then running bedtools v2.31.0[48] using the following command:

```
bedtools subtract -A -a {STR_test_set.bed} -b {catalog_i.bed} |
wc -l
```

We then divided the number of loci found to be unique to the STR test set by the overall size of the test set (250,262).

Identifying polymorphic TR loci in 78 T2T assemblies

To identify polymorphic TRs within haplotype-resolved T2T assemblies from 78 individuals for use as our TR test set and as the 4th source of TR loci for our TR catalog (**Table 1, row #4**), we employed the algorithm described in Weisburd et al.[28] Briefly, we performed assembly-to-hg38 alignments and variant detection for each individual by running dipcall v0.3 with default parameters.[49] Then, we filtered high-

confidence insertion and deletion variants to the subset that represented tandem repeat expansions or contractions. For an insertion or deletion allele to be considered a tandem repeat variant, its non-reference sequence plus its flanking reference sequences needed to consist of 3 or more repeats of some motif while spanning at least 9bp. We then merged per-sample TRs from the 78 individuals by running the merge_loci.py script provided in the str-analysis repo. The pipelines for running dipcall and generating the merged set of TR loci are implemented in the str-truth-set-v2 repo run_dipcall_pipeline.py and run_filter_vcf.py scripts.

Detecting All Perfect Repeats in the Reference Genome

To identify uninterrupted TR stretches in the reference genome, we located all sequences that spanned at least 9bp and consisted of at least three repeats of any 1-1000 bp motif. We implemented this method in the colab-repeat-finder GitHub repo perfect_repeat_finder.py script, and ran it as follows:

```
python3 perfect_repeat_finder.py --min-repeats 3 --min-span 9
--min-motif-size 1 --max-motif-size 1000  hg38.fa
```

Initially, we tried using TRF v4.09.1 for this purpose by setting its mismatch and indel penalties to prohibitively high values (ie. 10^7), and running it using the command:

```
trf409.macosx chr22.fa 2 10000000 10000000 80 10 2 2000 -h -ngs
```

However, when we compared TRF output for hg38 chr22 to that of perfect_repeat_finder.py, we found that TRF missed 1,355 (2%) out of the 67,638 perfect TRs detected by our approach. At the same time, our approach detected all perfect TRs identified by TRF. Loci missed by TRF had a variety of motifs and locus sizes, including the following examples: chr22:39,325,454-39,325,467 (GAG), chr22:22,778,396-22,778,417 (GATATA), chr22:50,530,014-50,530,023 (CGG), chr22:43,504,251-43,504,261 (TGA).

Variation plots

A variation plot (as shown in **Figure 3**) is a visualization of a matrix whose columns correspond to bases in some genomic region and whose rows correspond to sequenced samples. The element (□, □) of the matrix is the fraction of alternative bases observed at position □ in the sample □. The numerator of this fraction counts deleted bases, mismatched bases, and inserted bases (an insertion is assigned the reference

position of its anchor base). The denominator is given by the number of HiFi reads that span the entire region. The maximum value of the fraction is set to 1.0.

Detection of variation clusters with vclust

To determine the variation cluster (VC) that a given TR belongs to, we implemented a method called vclust, available on GitHub (https://github.com/PacificBiosciences/vclust). The method calculates the probability that each base surrounding a given TR belongs to the VC. It then iteratively extends the boundaries of the VC upstream and downstream by one base pair at a time until the probability that each flanking base belongs to a variation cluster drops below 0.5 (**Figure S3**). To calculate the VC probability for a given base (**Figure S3A**), we consider variation in a window starting at that base and extending 150 bp away from the repeat (**Figure S3B**). We discretize variation for each base of the window into six categories according to the fraction of observed alternative bases (≤0.10, ≤0.25, ≤0.75, ≤1.50, ≤5.00, and >5.00) producing a 150 element *variation vector* with entries in $\{0, \ldots, 5\}$. We then calculate the probability that the first base of the variation vector window □ belongs to the variation cluster using □(□□ | □) = □(□ | □□)□(□□) / (□(□ | □□)□(□□) + □(□ | □□□)□(□□□)). Here, the terms □(□ | □□) and □(□ | □□□) represent probabilities that the first base of the window □ belongs to a variation cluster or is outside of the variation cluster respectively. They are calculated according to **Figure S3D** and **S3E**. The terms □(□□□) and □(□□) are set to 0.58 and 0.42 respectively. The distributions in **Figure S3D** and **S3E** are defined through the following analysis: We randomly picked 50,000 TRs from our catalog, and then extracted the upstream and downstream flanking sequences of these TRs from 100 HPRC HiFi samples. The resulting sequences were aligned to the corresponding segments of the hg38 reference genome. If the base adjacent to the TR (rightmost base for the upstream flank and leftmost base for the downstream flank) was soft-clipped in more than half of the samples, we designated it as being in a variation cluster. We used the corresponding (discretized) variation windows to create the distributions depicted in **Figure S3D, E**. A locus was designated as a variation cluster if its boundary was extended by more than 5 bp in either direction. Overlapping variation clusters were then merged together.

TRGT LPS genotypes

Longest pure segments (LPS)[45] within repeat alleles were calculated using the recently developed TRGT-LPS tool (https://github.com/PacificBiosciences/trgt-lps). Briefly, TRGT-LPS finds copies of a given motif using a hidden Markov model (see TRGT

paper) and then calculates the longest stretch of consecutive copies of that motif, which is allowed to have at most one imperfect motif per 10 perfect motif occurrences.

Assembly consistency analysis

The assembly consistency analysis was performed as follows. We concatenated TR allele sequences produced by TRGT with 250 bp flanks extracted from the reference genome. We aligned the resulting sequences to the HG002 genome assembly with minimap2 2.24-r1122.[50] The edit distance between each allele sequence and the corresponding segment of the assembly was then used as a measure of consistency.

Acknowledgments

This work was supported in part by the Victorian State Government Operational Infrastructure Support and Australian Government National Health and Medical Research Council Independent Research Institute Infrastructure Support Scheme. BW and HR were supported by the National Human Genome Research Institute (NHGRI) under grant U01HG011755. LH is supported by the National Cancer Institute (NCI) under grant F30CA284847. HZJ and MG were partially supported by the National Human Genome Research Institute (NHGRI) under grant 1R01HG010149.

Data Availability

The Repeat Catalog is available on the Releases page of the tandem-repeat-catalog GitHub repo (https://github.com/broadinstitute/tandem-repeat-catalog).

The 100 HiFi samples from the Human Pangenome Reference Consortium are available under BioProject ID PRJNA850430 (https://www.ncbi.nlm.nih.gov/bioproject/730823) in SRA. TRGT allele calls for each of the individual samples are available from the authors upon request.

Code Availability

- https://github.com/broadinstitute/TRExplorer
  TRExplorer online portal client-side and server-side code

- https://github.com/broadinstitute/variation-clusters
  documentation and tutorials for computing variation clusters

- https://github.com/broadinstitute/tandem-repeat-catalogs
  scripts for generating the new repeat catalog described in this paper

- https://github.com/broadinstitute/colab-repeat-finder
  tool for detecting perfect repeats in nucleotide sequences

- https://github.com/broadinstitute/str-analysis
  utilities for filtering, annotating, and converting TR catalogs to a variety of formats

- https://github.com/broadinstitute/str-truth-set-v2
  pipelines for identifying TR variants through T2T-assembly-to-reference-genome alignment via dipcall, followed by filtering and post-processing steps[28]

- https://github.com/PacificBiosciences/vclust
  variation cluster analysis tool

- https://github.com/PacificBiosciences/trgt-lps
  TRGT companion tool that processes TRGT allele sequences to detect the longest pure segments (LPS)

Supplementary Information

Different definitions of the *PABPN1* locus

In the hg38 reference, the *PABPN1* locus locus begins with six GCGs (chr14:23,321,473 - 23,321,490), followed by three GCAs (chr14:23,321,491 - 23,321,499), followed by GCG·GGG·GCT·GCG. This sequence can be concisely represented as GCG[6]GCA[3]GCG[1]GGG[1]GCT[1]GCG[1]. Brais et al. (1998)[51] established that *PABPN1* expansions to 8 or more GCG repeats cause autosomal dominant oculopharyngeal muscular dystrophy (OPMD). Their study did not include the adjacent GCA[3]GCG[1] in the estimation of the pathogenic threshold, and thereby set locus boundaries at chr14:23,321,473 - 23,321,490. However, subsequent studies[7,52] and resources such as GeneReviews and STRchive[29] extended the boundaries to chr14:23,321,473 - 23,321,499, including GCA[3]GCG[1], and therefore adjusted the pathogenic threshold to 12 or more repeats. In the meantime, other resources such as the STRipy database[53] and gnomAD continued to use Brais et al.'s original locus boundaries and pathogenic threshold of 8. While these different definitions describe the same biological reality, the inconsistency creates the potential for inadvertent errors in OPMD diagnosis.

Supplementary Figures

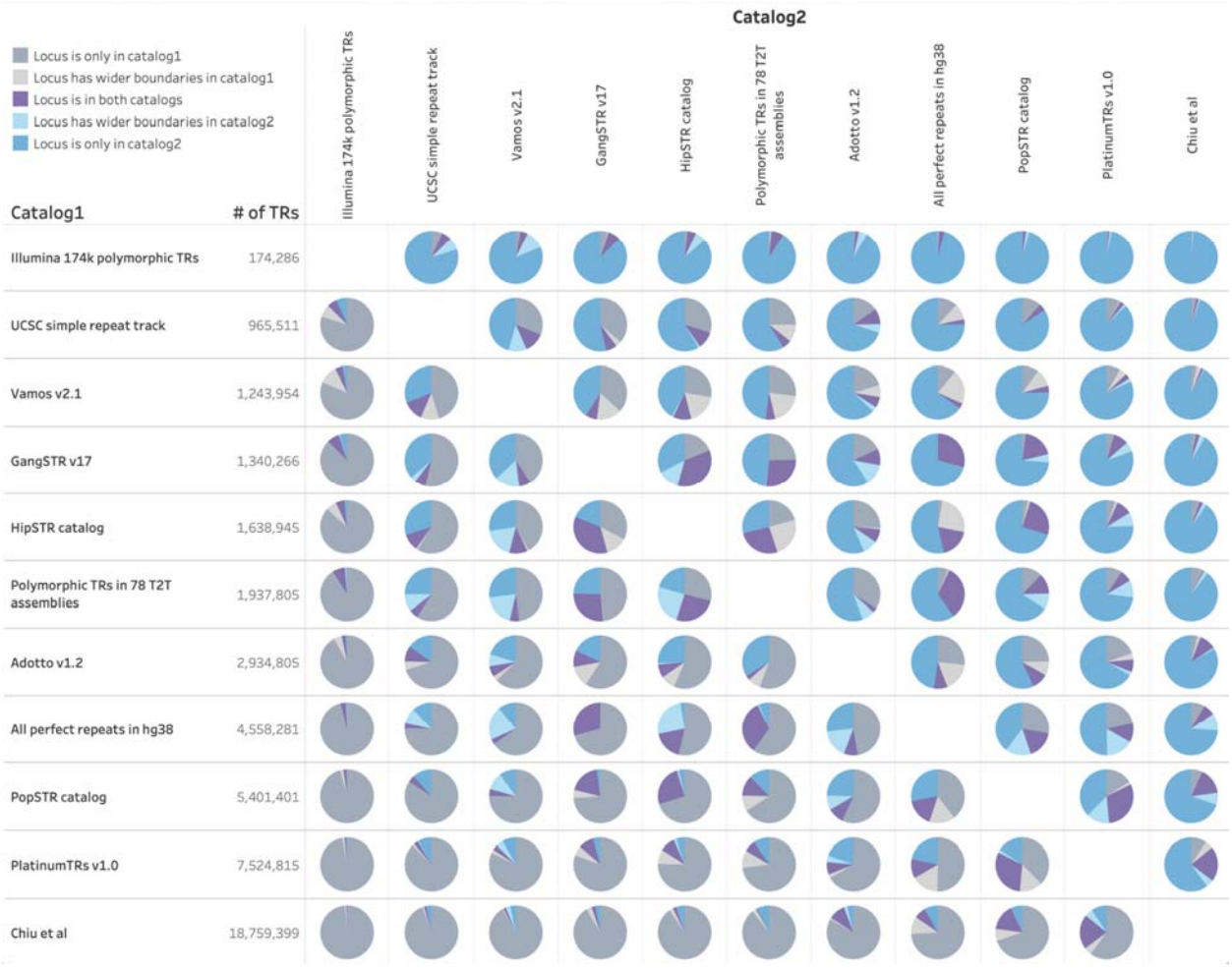

Supplementary Figure 1: Pairwise comparison of TR definitions in 11 catalogs. A locus was considered to be in both catalogs (purple) if the two locus definitions overlapped each other by at least 5%, specified the same motif, and differed in size by less than one motif length. Motif cyclic shifts and reverse complements (ie. CAG, AGC, GAC, CTG, TGC, GCT) were considered to be equivalent. Locus definitions with the same motif but wider boundaries in catalog 1 (light gray) or wider boundaries in catalog 2 (light blue) were counted separately.

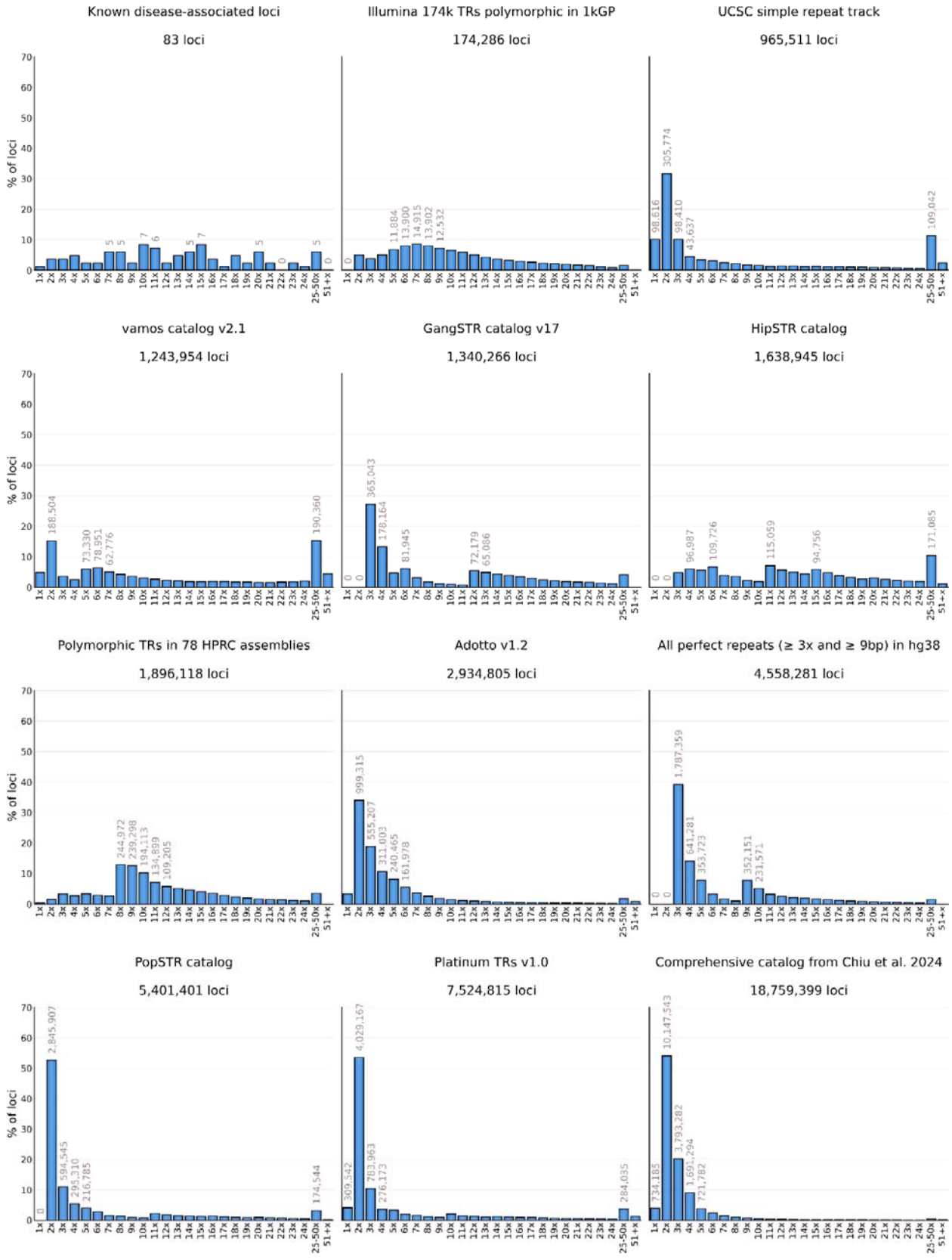
Known disease-associated loci
83 loci
Illumina 174k TRs polymorphic in 1kGP
174,286 loci
UCSC simple repeat track
965,511 loci
vamos catalog v2.1
1,243,954 loci
GangSTR catalog v17
1,340,266 loci
HipSTR catalog
1,638,945 loci
Polymorphic TRs in 78 HPRC assemblies
1,896,118 loci
Adotto v1.2
2,934,805 loci
All perfect repeats (≥ 3x and ≥ 9bp) in hg38
4,558,281 loci
PopSTR catalog
5,401,401 loci
Platinum TRs v1.0
7,524,815 loci
Comprehensive catalog from Chiu et al. 2024
18,759,399 loci
% of loci

Supplementary Figure 2: Reference locus size distributions in 12 existing TR catalogs. The horizontal axis represents the repeat copy number of each locus in the hg38 reference genome.

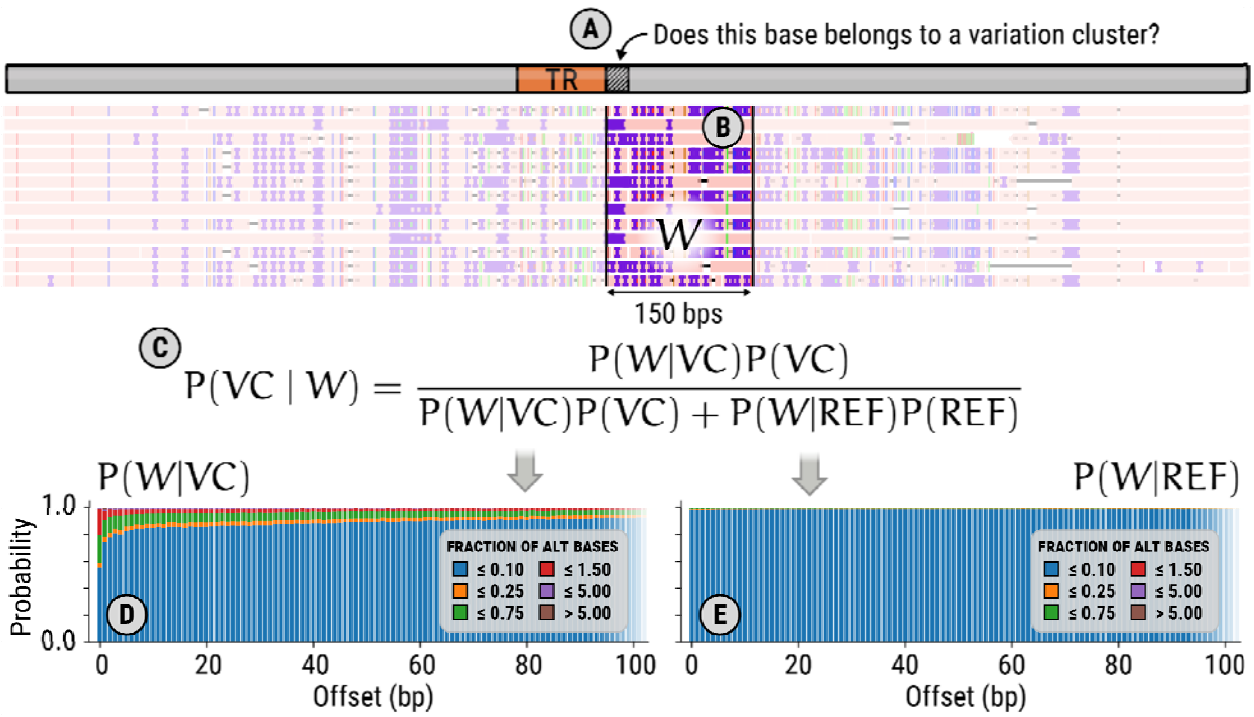

Supplementary Figure 3: Computing variation cluster boundaries. (A) The base being evaluated is adjacent to the tandem repeat. (B) The 150bp variation window that starts at the base under evaluation and extends away from the repeat. (C) The equation used to evaluate the probability that the first base of the window belongs to a variation cluster. (D) The model used to evaluate . (E) The model used to evaluate .

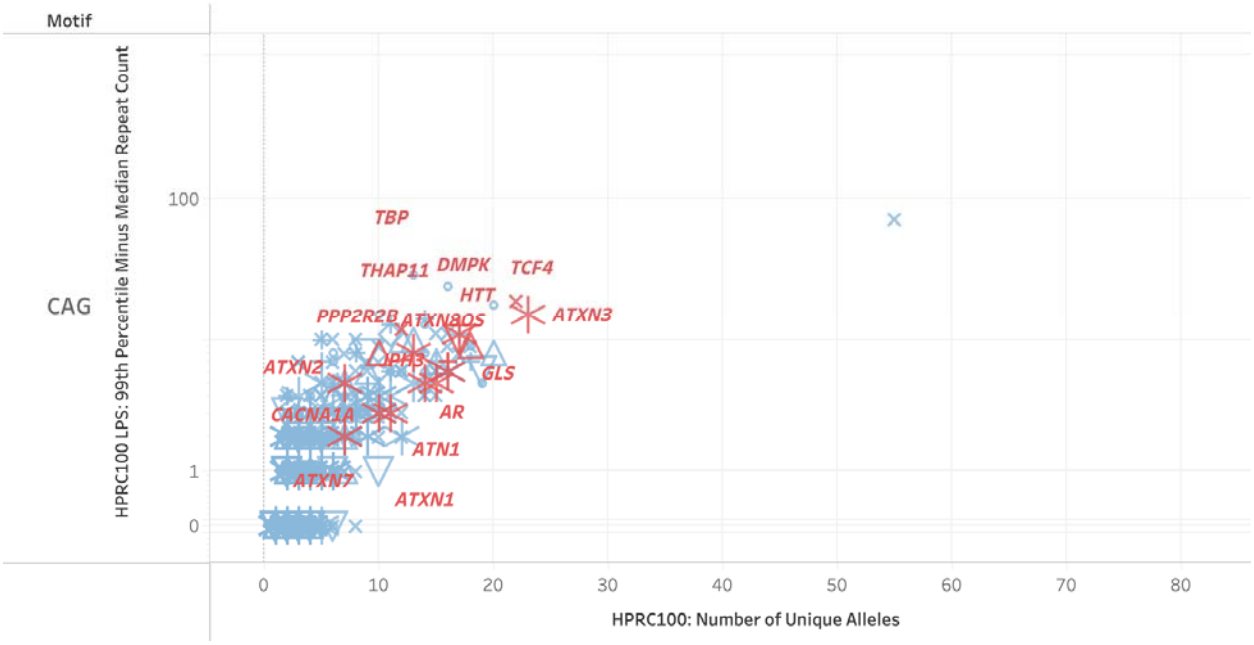
Motif
CAG
HPRC100 LPS: 99th Percentile Minus Median Repeat Count
100
1
0
TBP
THAP11
DMPK
TCF4
HTT
ATXN3
PPP2R2B
ATXN8OS
ATXN2
PPP3
GLS
CACNA1A
AR
ATN1
ATXN7
ATXN1
0
10
20
30
40
50
60
70
80
HPRC100: Number of Unique Alleles

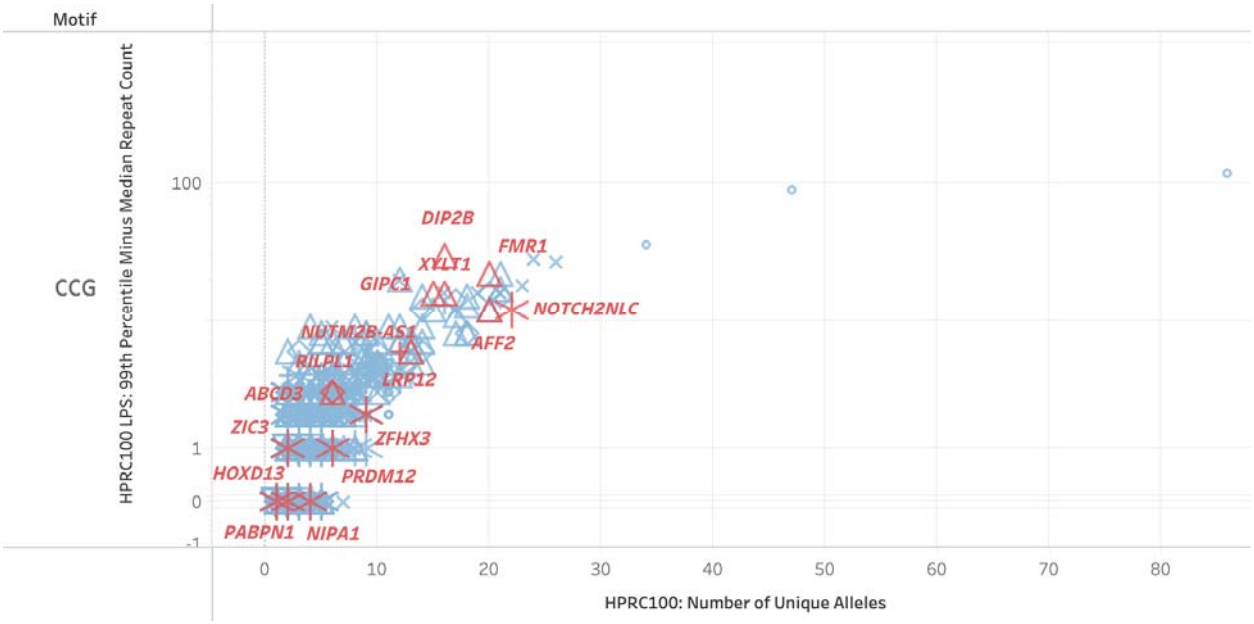
Motif
CCG
HPRC100 LPS: 99th Percentile Minus Median Repeat Count
100
1
0
-1
DIP2B
FMR1
XYLT1
GIPC1
NOTCH2NLC
NUTM2B-AS1
AFF2
RILPL1
LRP12
ABCD3
ZIC3
ZFHX3
HOXD13
PRDM12
PABPN1
NIPA1
0
10
20
30
40
50
60
70
80
HPRC100: Number of Unique Alleles

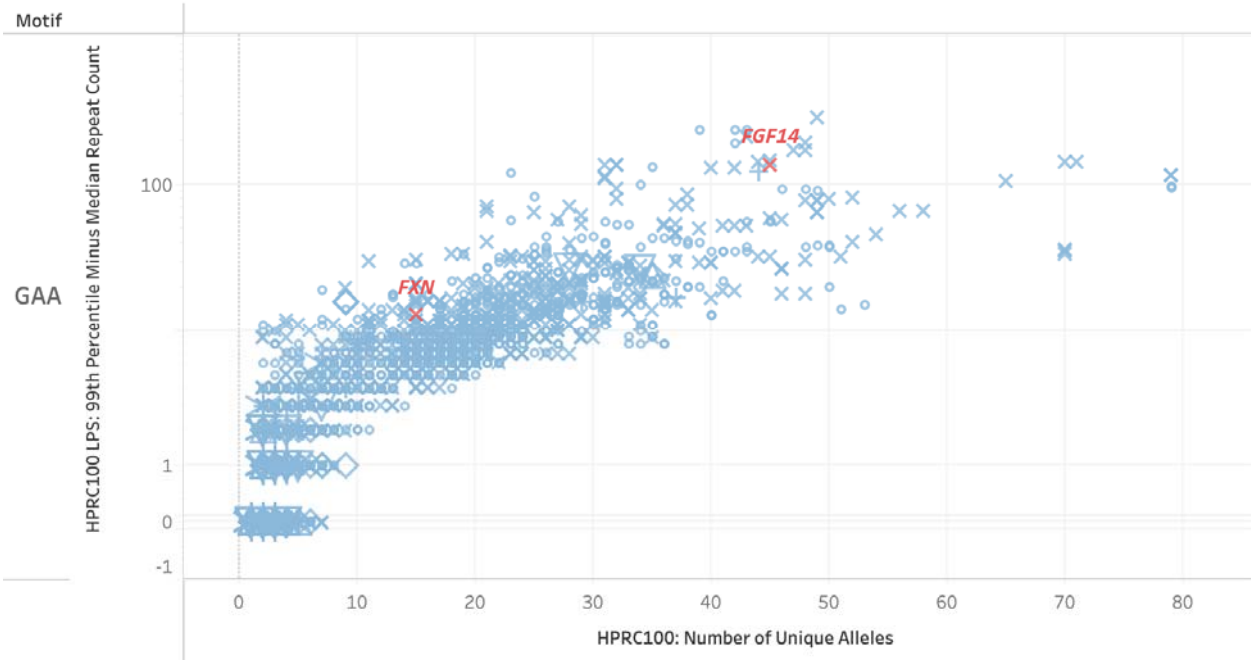
Motif
GAA
HPRC100 LPS: 99th Percentile Minus Median Repeat Count
100
1
0
-1
FGF14
FXN
0
10
20
30
40
50
60
70
80
HPRC100: Number of Unique Alleles

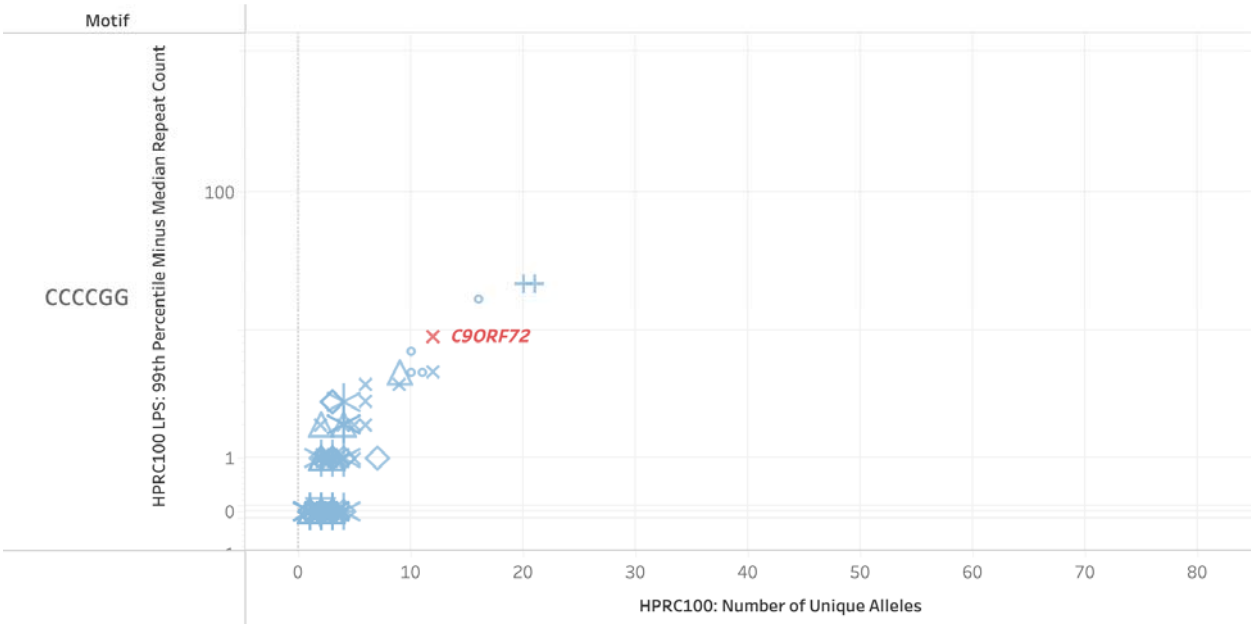
Motif
CCCCGG
HPRC100 LPS: 99th Percentile Minus Median Repeat Count
100
1
0
C9ORF72
0
10
20
30
40
50
60
70
80
HPRC100: Number of Unique Alleles

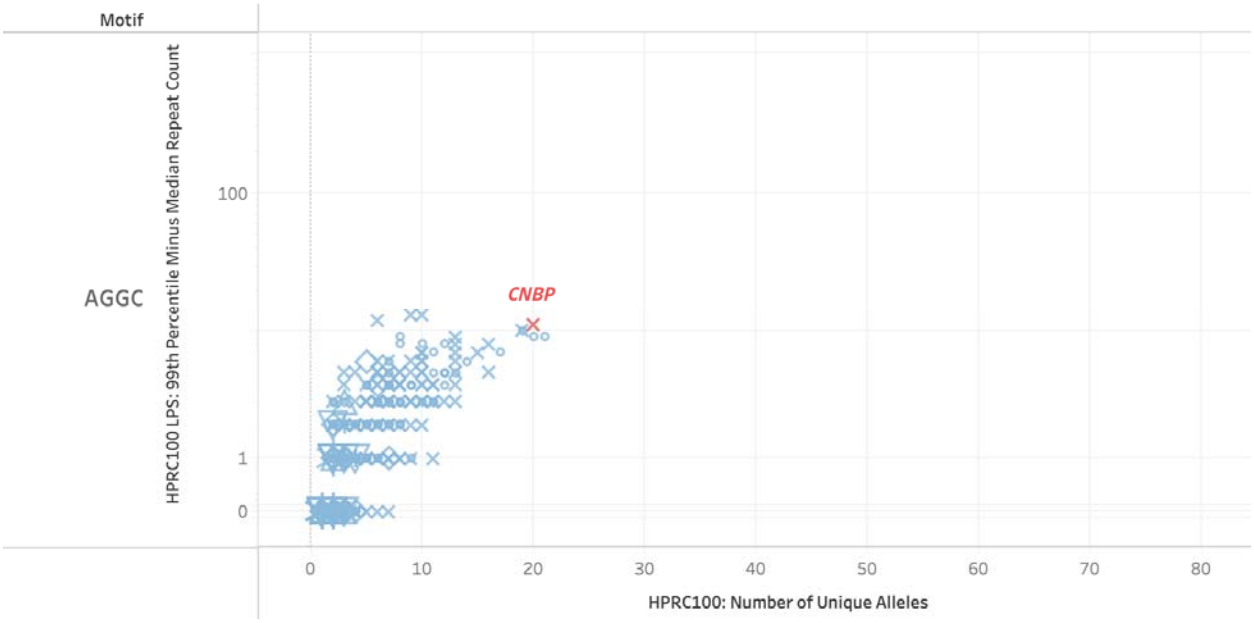
Motif
AGGC
HPRC100 LPS: 99th Percentile Minus Median Repeat Count
100
1
0
CNBP
0
10
20
30
40
50
60
70
80
HPRC100: Number of Unique Alleles

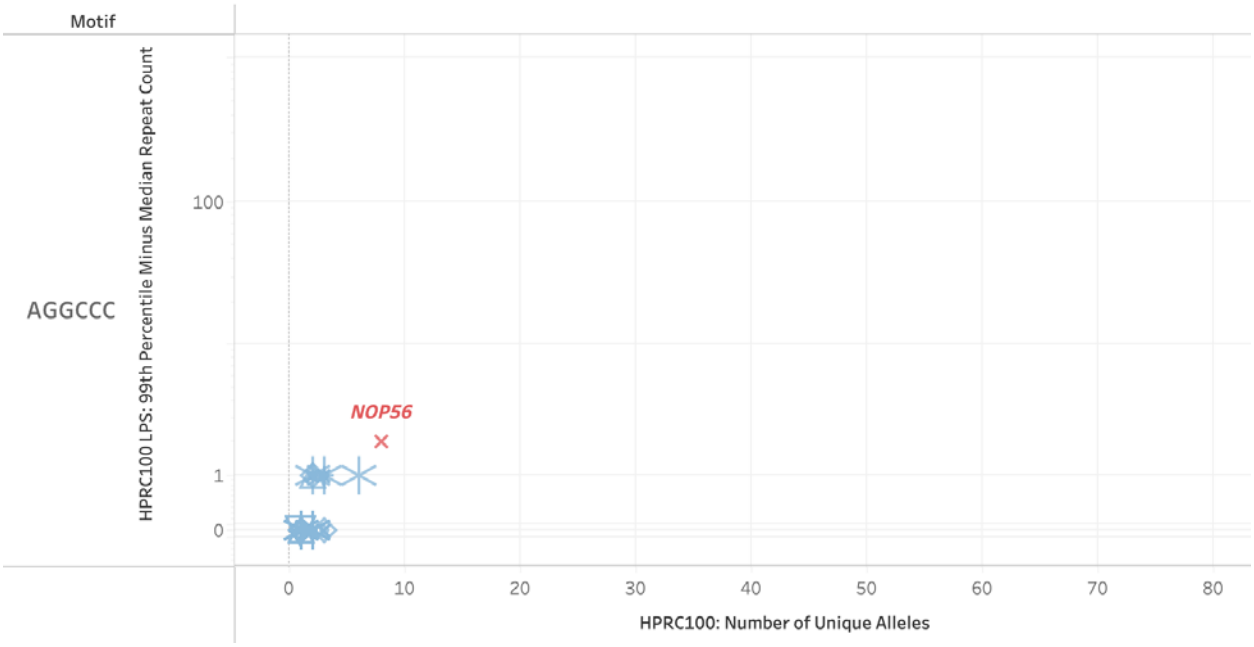
Motif
AGGCCC
HPRC100 LPS: 99th Percentile Minus Median Repeat Count
100
1
0
NOP56
0
10
20
30
40
50
60
70
80
HPRC100: Number of Unique Alleles

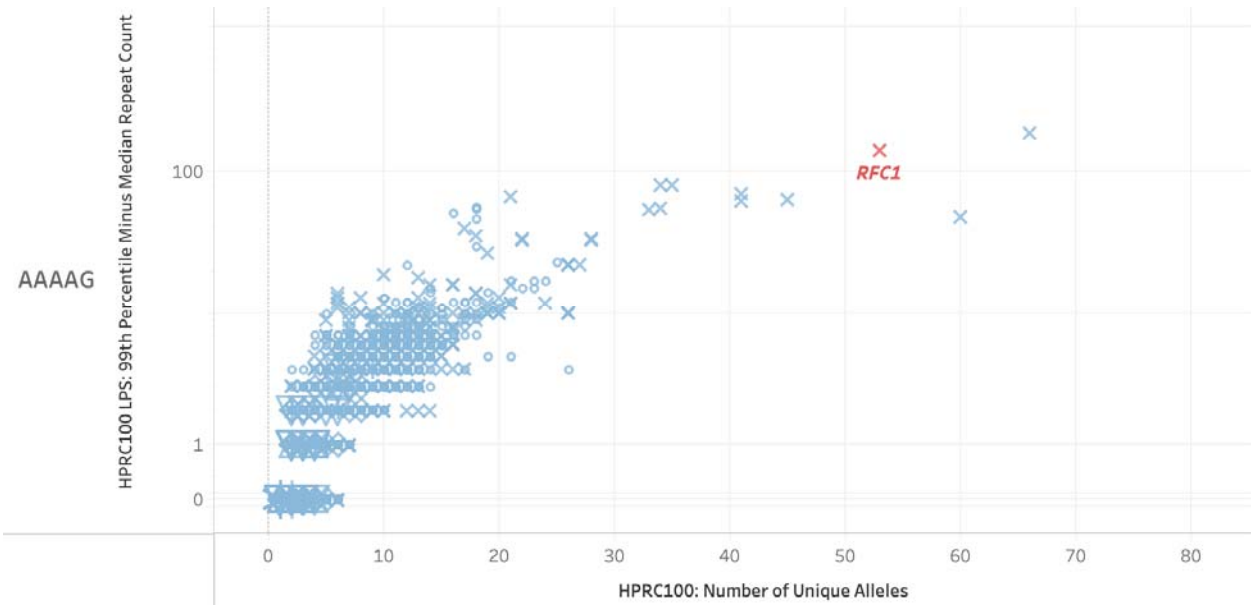

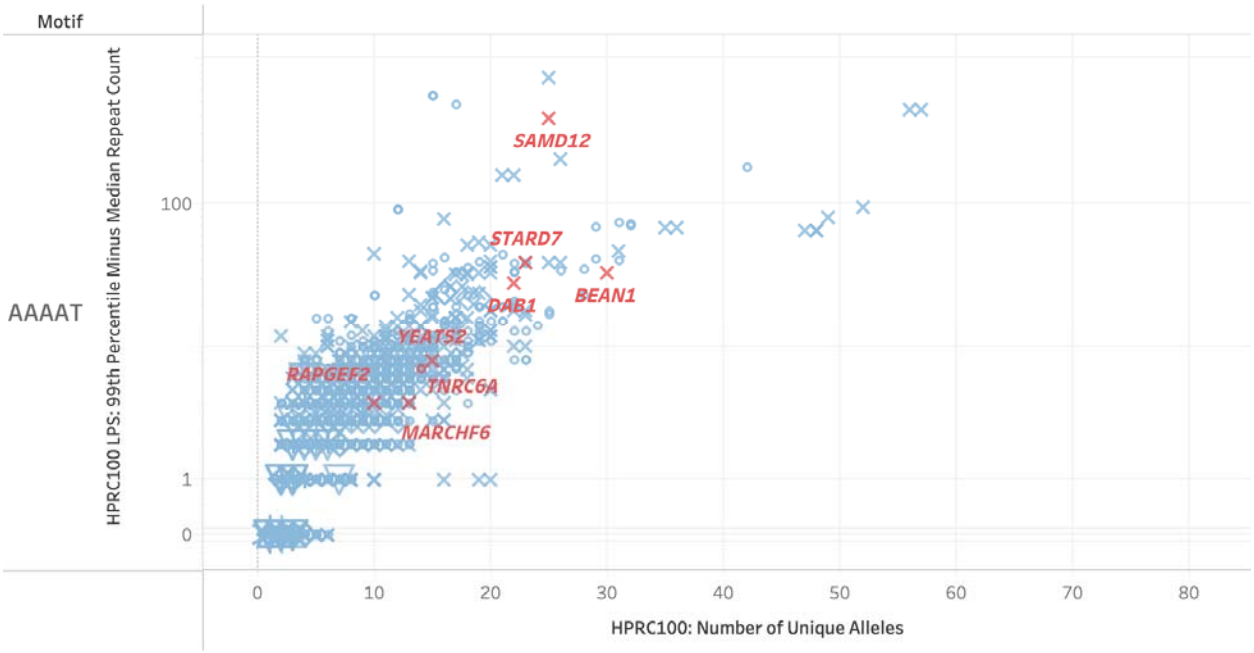

Known Disease-associated Loci

Other TR Loci

○ intergenic

✕ intron

+ non-coding exon

◇ promoter

△ 5′ UTR

▽ 3′ UTR

✱ CDS

Supplementary Figure 4: Comparison of locus polymorphism rates stratified by motif. Comparison of known disease-associated STR loci with all other loci in the catalog that share the same normalized motif (where shifted or reverse-complemented motifs such as CAG, AGC, GCA, TGC, etc. are considered to be the same). Each panel shows data for a different STR motif: (A) CAG (B) CCG (C) GAA (D) CCCCGG (E) AGGC (F) AGGCCC (G) AAAAG (H) AAAAT. Two metrics of polymorphism are shown on the x- and y- axis: the x-axis shows the number of observed TR allele sizes at a locus, while the y-axis shows the 99th percentile allele size minus the median allele size (in units of repeat counts) at a locus. The color is red for known disease-associated loci and blue for all other loci. Different shapes represent the gene region of each locus in Gencode v46. The polymorphism metrics were generated by running TRGT-LPS with the full TR catalog on 100 long-read HPRC samples from diverse populations.

Supplementary Tables

Supplementary Table 1: Per-locus annotations provided with the catalog. Some annotations such as GencodeGeneName are only available for a subset of TRs. The six annotation categories are: Basic locus properties derived from the catalog itself or the reference genome (green), mappability (orange), variation clusters (blue), whether this is a known disease-associated locus (red), gene annotations (yellow), locus variability and population allele frequencies (purple).

Supplementary Table 2: Summary of annotations at known disease-associated loci. This table lists the hg38 start (0-based) and end coordinates, motifs, gene regions based on Gencode v46, polymorphism rates (computed as the standard deviation of the TRGT-LPS repeat size distribution in 100 long-read samples from the HPRC), average mappability of the locus and flanking regions, whether the locus is embedded within a larger variation cluster (and if yes, how much larger it is than the TR locus), and finally, the number of other TR loci near this locus.

References

1. Steely, C. J., Watkins, W. S., Baird, L. & Jorde, L. B. The mutational dynamics of short tandem repeats in large, multigenerational families. *Genome Biol.* **23**, 253 (2022).
2. Porubsky, D. *et al.* A familial, telomere-to-telomere reference for human de novo mutation and recombination from a four-generation pedigree. *bioRxiv* (2024) doi:10.1101/2024.08.05.606142.
3. Mitra, I. *et al.* Patterns of de novo tandem repeat mutations and their role in autism. *Nature* **589**, 246–250 (2021).
4. Kristmundsdottir, S. *et al.* Sequence variants affecting the genome-wide rate of germline microsatellite mutations. *Nat. Commun.* **14**, 3855 (2023).
5. Fotsing, S. F. *et al.* The impact of short tandem repeat variation on gene expression. *Nat. Genet.* **51**, 1652–1659 (2019).
6. Hamanaka, K. *et al.* Genome-wide identification of tandem repeats associated with splicing variation across 49 tissues in humans. *Genome Res.* **33**, 435–447 (2023).

7. Depienne, C. & Mandel, J.-L. 30 years of repeat expansion disorders: What have we learned and what are the remaining challenges? *Am. J. Hum. Genet.* **108**, 764–785 (2021).
8. Hannan, A. J. Tandem repeats mediating genetic plasticity in health and disease. *Nat. Rev. Genet.* **19**, 286–298 (2018).
9. Dolzhenko, E. *et al.* ExpansionHunter Denovo: a computational method for locating known and novel repeat expansions in short-read sequencing data. *Genome Biol.* **21**, 102 (2020).
10. Dashnow, H. *et al.* STRling: a k-mer counting approach that detects short tandem repeat expansions at known and novel loci. *Genome Biol.* **23**, 257 (2022).
11. Fearnley, L. G., Bennett, M. F. & Bahlo, M. Detection of repeat expansions in large next generation DNA and RNA sequencing data without alignment. *Sci. Rep.* **12**, 13124 (2022).
12. Dolzhenko, E. *et al.* ExpansionHunter: a sequence-graph-based tool to analyze variation in short tandem repeat regions. *Bioinformatics* **35**, 4754–4756 (2019).
13. Mousavi, N., Shleizer-Burko, S., Yanicky, R. & Gymrek, M. Profiling the genome-wide landscape of tandem repeat expansions. *Nucleic Acids Res.* **47**, e90 (2019).
14. Ziaei Jam, H. *et al.* LongTR: genome-wide profiling of genetic variation at tandem repeats from long reads. *Genome Biol.* **25**, 176 (2024).
15. Dolzhenko, E. *et al.* Characterization and visualization of tandem repeats at genome scale. *Nat. Biotechnol.* (2024) doi:10.1038/s41587-023-02057-3.
16. Gymrek, M., Golan, D., Rosset, S. & Erlich, Y. lobSTR: A short tandem repeat profiler for personal genomes. *Genome Res.* **22**, 1154–1162 (2012).

17. Dashnow, H. *et al.* STRetch: detecting and discovering pathogenic short tandem repeat expansions. *Genome Biol.* **19**, 121 (2018).
18. Tankard, R. M. *et al.* Detecting expansions of tandem repeats in cohorts sequenced with short-read sequencing data. *Am. J. Hum. Genet.* **103**, 858–873 (2018).
19. Ren, J., Gu, B. & Chaisson, M. J. P. vamos: VNTR annotation using efficient motif sets. *bioRxiv* 2022.10.07.511371 (2022) doi:10.1101/2022.10.07.511371.
20. Kristmundsdottir, S., Eggertsson, H. P., Arnadottir, G. A. & Halldorsson, B. V. popSTR2 enables clinical and population-scale genotyping of microsatellites. *Bioinformatics* **36**, 2269–2271 (2020).
21. Willems, T. *et al.* Genome-wide profiling of heritable and de novo STR variations. *Nat. Methods* **14**, 590–592 (2017).
22. Kaivola, K. *et al.* Genome-wide structural variant analysis identifies risk loci for non-Alzheimer's dementias. *Cell Genom.* **3**, 100316 (2023).
23. Tanudisastro, H. A., Deveson, I. W., Dashnow, H. & MacArthur, D. G. Sequencing and characterizing short tandem repeats in the human genome. *Nat. Rev. Genet.* **25**, 460–475 (2024).
24. Genovese, L. M., Mosca, M. M., Pellegrini, M. & Geraci, F. Dot2dot: accurate whole-genome tandem repeats discovery. *Bioinformatics* **35**, 914–922 (2019).
25. Benson, G. Tandem repeats finder: a program to analyze DNA sequences. *Nucleic Acids Res.* **27**, 573–580 (1999).
26. *Docs/str_generation.md at Master · Illumina/RepeatCatalogs*. (Github).
27. Chiu, R., Rajan-Babu, I.-S., Friedman, J. M. & Birol, I. A comprehensive tandem

repeat catalog of the human genome. *medRxiv* (2024) doi:10.1101/2024.06.19.24309173.

28. Weisburd, B., Tiao, G. & Rehm, H. L. Insights from a genome-wide truth set of tandem repeat variation. (2023) doi:10.1101/2023.05.05.539588.
29. Hiatt, L. *et al.* STRchive: a dynamic resource detailing population-level and locus-specific insights at tandem repeat disease loci. *medRxiv* (2024) doi:10.1101/2024.05.21.24307682.
30. Hoyt, S. J. *et al.* From telomere to telomere: The transcriptional and epigenetic state of human repeat elements. *Science* **376**, eabk3112 (2022).
31. Ziaei Jam, H. *et al.* A deep population reference panel of tandem repeat variation. *Nat. Commun.* **14**, 6711 (2023).
32. Pellerin, D. *et al.* A common flanking variant is associated with enhanced stability of the FGF14-SCA27B repeat locus. *Nat. Genet.* **56**, 1366–1370 (2024).
33. Rajan-Babu, I.-S., Dolzhenko, E., Eberle, M. A. & Friedman, J. M. Sequence composition changes in short tandem repeats: heterogeneity, detection, mechanisms and clinical implications. *Nat. Rev. Genet.* **25**, 476–499 (2024).
34. Dominik, N. *et al.* Normal and pathogenic variation of RFC1 repeat expansions: implications for clinical diagnosis. *Brain* **146**, 5060–5069 (2023).
35. Ibañez, K. *et al.* Whole genome sequencing for the diagnosis of neurological repeat expansion disorders in the UK: a retrospective diagnostic accuracy and prospective clinical validation study. *Lancet Neurol.* **21**, 234–245 (2022).
36. van der Sanden, B. P. G. H. *et al.* Systematic analysis of short tandem repeats in 38,095 exomes provides an additional diagnostic yield. *Genet. Med.* **23**, 1569–1573

(2021).

37. Cui, Y. *et al.* A genome-wide spectrum of tandem repeat expansions in 338,963 humans. *Cell* **187**, 2336–2341.e5 (2024).
38. Gall-Duncan, T., Sato, N., Yuen, R. K. C. & Pearson, C. E. Advancing genomic technologies and clinical awareness accelerates discovery of disease-associated tandem repeat sequences. *Genome Res.* **32**, 1–27 (2022).
39. Rautiainen, M. *et al.* Telomere-to-telomere assembly of diploid chromosomes with Verkko. *Nat. Biotechnol.* **41**, 1474–1482 (2023).
40. Rhie, A. *et al.* The complete sequence of a human Y chromosome. *Nature* **621**, 344–354 (2023).
41. Frankish, A. *et al.* GENCODE: reference annotation for the human and mouse genomes in 2023. *Nucleic Acids Res.* **51**, D942–D949 (2023).
42. O'Leary, N. A. *et al.* Reference sequence (RefSeq) database at NCBI: current status, taxonomic expansion, and functional annotation. *Nucleic Acids Res.* **44**, D733–45 (2016).
43. Morales, J. *et al.* A joint NCBI and EMBL-EBI transcript set for clinical genomics and research. *Nature* **604**, 310–315 (2022).
44. Marco-Sola, S., Sammeth, M., Guigó, R. & Ribeca, P. The GEM mapper: fast, accurate and versatile alignment by filtration. *Nat. Methods* **9**, 1185–1188 (2012).
45. Danzi, M. C. *et al.* Detailed tandem repeat allele profiling in 1,027 long-read genomes reveals genome-wide patterns of pathogenicity. *bioRxivorg* (2025) doi:10.1101/2025.01.06.631535.
46. English, A. *et al.* Benchmarking of small and large variants across tandem repeats.

bioRxiv (2023) doi:10.1101/2023.10.29.564632.

47. Gu, B. & Chaisson, M. J. P. TRCompDB: A reference of human tandem repeat sequence and composition variation from long-read assemblies. *bioRxiv* 2024.08.07.607105 (2024) doi:10.1101/2024.08.07.607105.
48. Quinlan, A. R. & Hall, I. M. BEDTools: a flexible suite of utilities for comparing genomic features. *Bioinformatics* **26**, 841–842 (2010).
49. Li, H. *et al.* A synthetic-diploid benchmark for accurate variant-calling evaluation. *Nat. Methods* **15**, 595–597 (2018).
50. Li, H. Minimap2: pairwise alignment for nucleotide sequences. *Bioinformatics* **34**, 3094–3100 (2018).
51. Brais, B. *et al.* Short GCG expansions in the PABP2 gene cause oculopharyngeal muscular dystrophy. *Nat. Genet.* **18**, 164–167 (1998).
52. Smith, I. C. *et al.* Emerging and established biomarkers of oculopharyngeal muscular dystrophy. *Neuromuscul. Disord.* **33**, 824–834 (2023).
53. Halman, A., Dolzhenko, E. & Oshlack, A. STRipy: A graphical application for enhanced genotyping of pathogenic short tandem repeats in sequencing data. *Hum. Mutat.* **43**, 859–868 (2022).